Available online at www.sciencedirect.com

ScienceDirect

IFAC Papers Online CONFERENCE PAPER ARCHIVE

IFAC PapersOnLine 50-1 (2017) 14692–14697

Excitation force estimation and forecasting for wave energy applications

Garcia-Abril, M. * **Paparella, F.** ** **Ringwood, J. V.** ***

Centre for Ocean Energy Research (COER), Maynooth University, Ireland

* *e-mail: marina10_92@hotmail.com*
** *e-mail: francesco.paparella.2014@mumail.ie*
*** *e-mail: john.ringwood@eeng.nuim.ie*

Abstract: The implementation of the majority of energy maximising control strategies requires the knowledge of the wave excitation force experienced by the wave energy converter (WEC). In addition, many optimal numerical control strategies also require future knowledge, or a forecast, of future values of the excitation force. This paper examines both the excitation force estimation and forecasting problem for a heaving buoy wave energy device. In particular, a Kalman filter is used to estimate excitation force, where the wave force model is comprised of a set of oscillators at discrete frequencies. The forecasting algorithm consists of an autoregressive model, where the value of prefiltering, in terms of forecasting performance, is evaluated. The paper provides a level of sensitivity analysis of the estimation and forecasting performance to variations in sampling period, sea spectral shape factor and prediction horizon. Results demonstrate that the achievable performance of the estimator/forecaster is consistent with the broad requirements of numerical optimal WEC control strategies (Fusco and Ringwood (2012)), which depends on the characteristics of the radiation impulse response.

Keywords: Excitation force, prediction, estimation, Kalman filter, energy maximization.

1. INTRODUCTION

During recent decades, new types of energy extraction methods have been developed in order to supply the increasing energy demand of human activities. One of the natural resources with a higher technical potential is wave energy, being the renewable energy with the highest energy density per unit area (Kerrigan and Ge (2008)). Wave energy is converted in mechanical or electrical energy through Wave Energy Converters (WECs).

In the wave energy scenario, several control strategies have been developed to maximize the power extracted by a WEC. However, most of the control strategies requires the knowledge of the wave excitation force acting upon the wet surface of the device. It has been proved that the effectiveness of different real-time control strategies depends on the prediction of the future wave elevation or wave excitation force acting on the device (Falnes (2007), Fusco and Ringwood (2011), Fusco and Ringwood (2013), Bacelli et al. (2013), Ringwood et al. (2014)). Some others developed sub-optimal control schemes that minimize or eliminate the need of knowing excitation forces (Falcao (2008)). Nevertheless, for the vast majority of the future knowledge of the wave excitation force is an essential requirement to maximize the energy extraction from the WEC. The optimal energy extraction is mandatory in order to reach the economic viability of wave energy (Fusco and Ringwood (2012), Peñalba Retes et al. (2015)).

The wave excitation force can be directly measured by using pressure sensors displaced on the wet surface of the device (Abdelkhalik et al. (2016)). However, a more practical solution can be to estimate the excitation force through a Kalman filter which takes the motion of the device as the input. The information on the motion of the device is easier to obtain than the pressure acting upon the device. Motion sensors are easy and cheap to install (Nord et al. (2015)). Furthermore, in order to implement the real-time control of a WEC, both the motion of the device and the knowledge of the excitation force are required. Therefore, the estimation of the excitation force through a Kalman filter allows to realize a real-time control strategy which is based only on the motion of the device, yielding to a more cost effective solution than using additional pressure sensors.

In the literature, works on the estimation of the excitation force experienced by the WEC can be found in Ling and Batten (2015), Abdelrahman et al. (2016). For the prediction of the excitation force, an autoregressive model can be applied (Fusco and Ringwood (2010b)). The forecasting horizon required by the real-time control depends on the characteristics of the impulse response of the radiation damping of the device (Fusco and Ringwood (2012)).

In this paper, an algorithm for the excitation force estimation based on the Kalman filter has been developed. Furthermore, an autoregressive model is fitted to the estimated excitation force and used to predict its future values.

10.1016/j.ifacol.2017.08.2499

This work is differentiated from others by:

- Consideration of the WEC's motion as the measurements.
- Prediction of the excitation force instead of the water surface elevation.
- Inclusion of white noise in the WEC's dynamics and in the measurements.
- Optimisation of the forecaster model for sampling time, peak shape factor and horizon time.

In this paper, the estimation of the excitation force is based on motion sensors only, as it provides a more economical and simpler solution than the direct measurement of the excitation force with pressure sensors. The white noise is included in the dynamics of the WEC in order to take into account the uncertainty associated with the modeling errors of the excitation force. Furthermore, the problem of forecasting of the excitation force is considered instead of the forecasting of the wave elevation (Fusco and Ringwood (2013), Hwang et al. (2009)), as the real-time control of a WEC requires the future excitation force in order to maximize the extracted energy. Also the influence of the sampling time and the peak-shape factor of the spectrum of the wave on the accuracy of the forecasting model is considered.

In Section 2, a specific geometry for the WEC is considered and its hydrodynamic model is derived in order to simulate the device for different waves conditions. In Section 3, the estimator for the excitation force is introduced while, in Section 4, the prediction model is presented. In Section 5, the performances of the predictor for different sea states and forecasting horizons are considered. Finally, in Section 6, conclusions are drawn for the device considered.

2. WAVE ENERGY CONVERTER MODEL

A cylindrical buoy has been considered as an example of WEC in this paper. The device is axisymmetric and it has a uniform cross-sectional area, so that linear potential theory can be applied to derive the hydrodynamic model of the device. It is assumed that the device only moves in the heave (vertical) direction. Device dimensions are shown in Table 1:

Table 1. Parameters of WEC model

Radius, r	5.0 m
Length, L	10.0 m
Draft, h	5.0 m
Mass, m	4 x 10^5 kg

The hydrodynamic model is based on linear potential theory, the fluid to be inviscid, and the flow to be irrotational and incompressible. Under these assumptions the hydrodynamic forces acting on the body consist of the hydrostatic force $K_H z$, the excitation force F_e, the added mass inertial force $A_\infty \ddot{z}$ and the radiation force F_{rad}. The dynamic model of the device is given as follows:

$$m\ddot{z} = -K_H z + F_e - A_\infty \ddot{z} - F_{Rad} + F_{PTO} \quad (1)$$

where the excitation force has been defined as it follows:

$$F_e = \int_{-\infty}^{+\infty} K_{Ex}(t-\tau)\eta(\tau)d\tau \quad (2)$$

and the radiation force:

$$F_{rad} = \dot{z}b \quad (3)$$

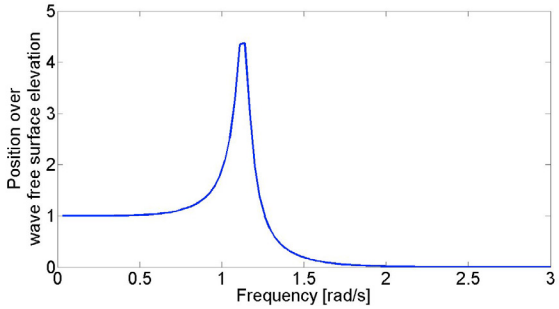

Fig. 1. Frequency response of the WEC

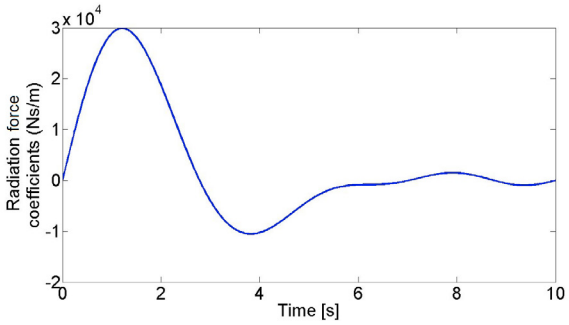

Fig. 2. Radiation impulse response.

The parameters used in eqs, (1)-(3) represents: the mass of the device (m), the vertical motion (z), the damping coefficients (K_H) and the added mass (A_∞).

Some previous works had used the convolution integral in order to obtain the radiation force Ling and Batten (2015). It can be shown that the estimator performance are not affected by the use of a simplified model as in eq. (3) rather than the convolution integral for the radiation force.

In this work, no Power Take-Off (PTO) force is considered in the dynamic model of the device, since the aim of the paper is to provide an algorithm for the estimation the excitation force which does not depend on the type of PTO used to extract energy from the device. Nevertheless, as the PTO force represents an input to the WEC, the PTO force can be easily included in the dynamics of the estimator model, without affecting the performances of the estimator. The hydrodynamic parameters are obtained with the software WAMIT (Tobergte and Curtis (2013)).

In Fig. 1 the frequency response of the WEC is shown: this plot is exclusively dependent on the device geometry and provides the natural frequency response of the WEC.

The added-mass and the radiation damping coefficients are frequency-dependent and they are shown in Fig. 2 and Fig. 3, respectively.

3. EXCITATION FORCE ESTIMATION

The excitation force can be measured directly or estimated. In the first case, pressure sensors would be placed on the WEC wet-surface to monitor the excitation force: this could be expensive and cumbersome. In the second case, the excitation force is estimated from the measurement of other variables that are affected by the excitation force, e.g. position and velocity of the WEC. During the

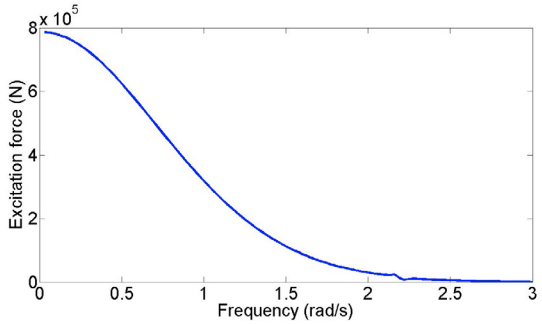

Fig. 3. Frequency response of the excitation force.

following section a Kalman Filter (KF) is presented, making use of measurements of position and velocity of the device, for estimating the real-time excitation forces acting on the wet-surface of the WEC.

The KF is an optimal linear estimator. The formulation used in this work is based on Lewis et al. (2008), so a dynamical system is described as it follows, considering white noise in the process and in the measurements:

$$\hat{s}_{k+1} = A\hat{s}_k + Bu_k + Gw_k \tag{4a}$$
$$z_k = H\hat{s}_k + v_k \tag{4b}$$
$$w_k \ (0, Q) \tag{4c}$$
$$v_k \ (0, R) \tag{4d}$$

where $\hat{s}_k$ represents the systems estimated states (position, velocity, excitation force and derivative of the excitation force), z_k the measurements obtained from the simulation (position and velocity of the vertical WEC motion), w_k and v_k are the white noise present in the process and in the measurement, respectively, and both are assumed to be stationary. In this work, there is no control input, denoted by u_k, so the second term of the eq. (4a) is zero. The capital letters represent the constant matrices of appropriate dimension: A defines the dynamic of the system, H is the measurements matrix, G is the weighting matrix for the state errors, whereas Q and R represents the covariance matrices of the white noise considered in the process and the measurements, respectively. The Q and R matrix are chosen in order to provide a trade-off between the accuracy and the noise level of the estimation of the excitation force. While Q represents the variance of the noise on the measurements of position and velocity, R values are appropriately tuned so that the noise level in the estimation of the excitation force is acceptable and the estimation rapidly converges to the real value of the excitation force.

The KF process has two steps Lewis et al. (2008): the prediction or time update (TU) and the correction or measurement-update (MU). In the first step, the algorithm estimates the variables with some uncertainty P, which is the effect of the system dynamics. Then, the sensors provide the next real measurement (also with some error), so that the previous estimate is improved by the direct observation.

KF *a priori* recursive formulation (TU):

$$P^-_{k+1} = AP_kA^T + GQG^T \tag{5a}$$
$$\hat{s}^-_{k+1} = A\hat{s}_k \tag{5b}$$

KF *a posteriori* estimation (MU):

$$K_{k+1} = P^-_{k+1}H^T(HP^-_{k+1}H^T + R)^{-1} \tag{6a}$$
$$P_{k+1} = (I - K_{k+1}H)P^-_{k+1} \tag{6b}$$
$$\hat{s}_{k+1} = \hat{s}^-_{k+1} + K_{k+1}(z_{k+1} - H\hat{s}^-_{k+1}) \tag{6c}$$

In equations (6), the Kalman gain K_{k+1} is the residual weighting coefficient, which provides an optimal weighting between the model and the measurements. The TU generally increases the covariance error due to the injection of uncertainty by the process noise w_k, whereas the MU decreases the error covariance by adding the measurement information.

The excitation force has an oscillating nature, so an harmonic oscillator model with an assumed wave frequencies ω_i is used to describe the excitation force. For the KF developed in this paper, the representative frequencies ω_i are assumed to be constant:

$$\begin{bmatrix} \dot{s} \\ \ddot{s} \\ \dot{\hat{F}}_e \\ \ddot{\hat{F}}_e \end{bmatrix} = \begin{bmatrix} 0 & 1 & 0 & 0 \\ \frac{-K_H}{m+A_\infty} & \frac{-b}{m+A_\infty} & \frac{1}{m+A_\infty} & 0 \\ 0 & 0 & 0 & I \\ 0 & 0 & -\Omega^2 & 0 \end{bmatrix} \begin{bmatrix} s \\ \dot{s} \\ \hat{F}_e \\ \dot{\hat{F}}_e \end{bmatrix} + \begin{bmatrix} 0 & 0 & 0 & 0 \\ 0 & 0 & 0 & 0 \\ 0 & 0 & 1 & 0 \\ 0 & 0 & 0 & 1 \end{bmatrix} w \tag{7a}$$

$$\begin{bmatrix} z \\ \dot{z} \end{bmatrix} = \begin{bmatrix} 1 & 0 & 0 & 0 \\ 0 & 1 & 0 & 0 \end{bmatrix} \begin{bmatrix} s \\ \dot{s} \\ \hat{F}_e \\ \dot{\hat{F}}_e \end{bmatrix} + v \tag{7b}$$

where I corresponds to the identity matrix and Ω is a diagonal matrix with the fixed frequencies:

$$\Omega = \begin{bmatrix} \omega_1 & 0 & 0 \\ 0 & \omega_2 & 0 \\ \vdots & \ddots & \vdots \\ 0 & 0 & \omega_i \end{bmatrix} \tag{8}$$

Considering more frequencies gives a more accurate result, but it also increases the problem complexity. The number of frequencies is related to the nature of the JONSWAP spectrum. A narrow spectrum requires a smaller number of fixed frequencies than a broad spectrum.

Eq. (7) must be discretised in order to implement eqs. (5) to (6). The covariance matrix of the state P in equation (5a) is initialized with rather large values since the initial estimate for the excitation force is characterized by a high degree of uncertainty. In particular, in the matrix P, the initial value for the covariance of the excitation force is 110^5 N^2.

In case the frequencies of the excitation force are not assumed to be fixed, but rather they change with time, the estimation problem become nonlinear and an EKF can be applied (Fusco and Ringwood (2010b)). The main differences between the regular KF and the EKF is that the frequencies considered in the KF are fixed, whereas, in the EKF, the frequencies are variables and can adapt to irregular waves.

While the KF correctly estimates the excitation force for both regular and irregular waves, the EKF provides an accurate estimation of the excitation force for regular

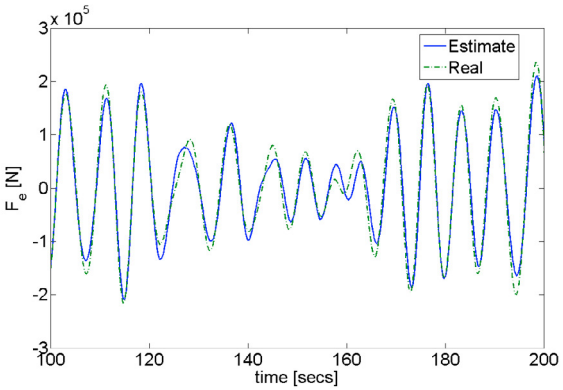

Fig. 4. Real and estimated excitation force.

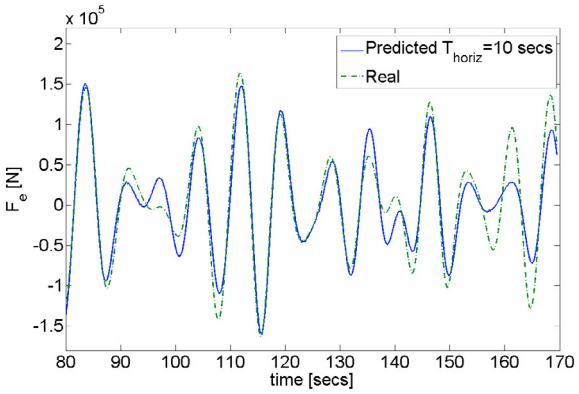

Fig. 5. Real and predicted excitation force.

waves only for an initial guess of the variable frequency sufficiently close to the real frequency of the wave. For irregular waves, the estimation of the excitation force provided by the EKF quickly diverges from the real excitation forces, regardless of the values for the Q and R matrices. However, the EKF is going to be further investigated and included in future works.

In Figure 4, the comparison between the real and estimated excitation force is made in the time domain.

4. PREDICTION MODEL

The prediction model is fitted to the estimation of the excitation force obtain in Section 3 and is used to predict its future values. The prediction model is an AutoRegressive (AR) model which is given as follows:

$$x_k^* = [\hat{F}_e(k)\hat{F}_e(k-1)...\hat{F}_e(k-n+1)] \quad (9a)$$

$$\hat{a}_k = [\hat{a}_1\hat{a}_2...\hat{a}_n]^T \quad (9b)$$

$$\bar{F}_e(k+1|k) = x_k^*\hat{a}_k \quad (9c)$$

The prediction accuracy can be measured by using the goodness-of-fit (GoF), which is a quality criteria linked to the standard deviation (Laurent (2016)), where n represents step-prediction for obtaining the horizon length and the intervals k are identical to the sampling time.

$$F(n) = (1 - \frac{\sqrt{\sum_k [F_e(k+n) - \bar{F}_e(k+n|k)]^2}}{\sqrt{\sum_k \bar{F}_e(k)^2}})100\% \quad (10)$$

Obtaining a value of $F(n) = 100\%$ means that the excitation force has been perfectly predicted in n steps into the future. The accuracy of the prediction is higher when the system bandwidth is narrow (Fusco and Ringwood (2010a)). Note that, the real values of the excitation force are obtained using the linear wave theory and no PTO taken into account.

In Figure 5, the comparison between the real and predicted excitation force is made in the time domain.

5. RESULTS & DISCUSSION

In this section, the performances of the estimation and prediction models are shown for different sea state and forecasting horizon.

The JONSWAP spectrum $E_{JONSWAP}(f)$ is used to reproduce the waves conditions. The spectrum of the wave

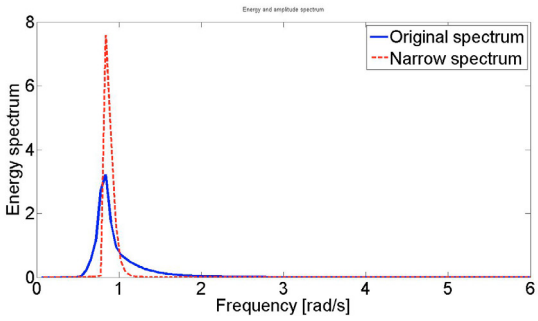

Fig. 6. JONSWAP spectrum

can be obtained from measurements of the wave elevation time series. The JONSWAP spectrum is obtained by multiplying the Pierson-Moskowitz $E_{PM}(f)$ spectrum with a 'peak enhancement' factor (Hasselmann et al. (1973)):

$$E_{JONSWAP}(f) = E_{PM}(f)\gamma^{exp[-\frac{(f-f_p)^2}{2\sigma^2 f_p^2}]} \quad (11)$$

For realistic sea-states the peak shape parameter $\gamma = 3.3$, $\sigma_a = 0.07$ ($f \leq f_m$) and $\sigma_b = 0.09$ ($f > f_m$) (as referenced in Monk et al. (2013), Paparella et al. (2015) for Pico Island, which has a narrow-banded frequency spectrum). The peak shape parameters characterize the properties of the narrow spectral peak and they accept some variability on their values (in Hasselmann et al. (1973) is shown that γ could reach values of 10^3 even if they are usually compressed between 1 and 7, as related in Ochi (1998)).

When modifying the characteristics of the considered spectrum, changes apply for the simulation and the estimation processes. The simulation describes the sea-state of the selected region and the estimation adapts its procedure to the wave spectrum of the location.

It is correct to see that when the JONSWAP spectrum has a narrower peak, the frequencies taken into account will be reduced. Dealing with less frequencies decreases the complexity of the problem, so the goodness-of-fit for narrow spectra is higher. In the actual work, four representative frequencies of the spectrum has been chosen. The differences between the typical spectrum for $\gamma = 3.3$ and the narrowest for $\gamma = 250$ are shown in Fig. 6.

The present results have been computed for a selected sea-state of significant wave height of $H_S = 1.5$m and peak

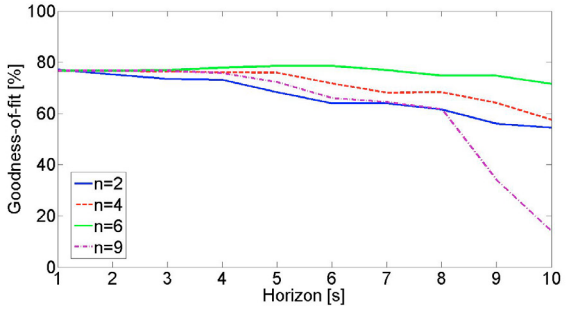

Fig. 7. GoF for different prediction orders along the required horizon

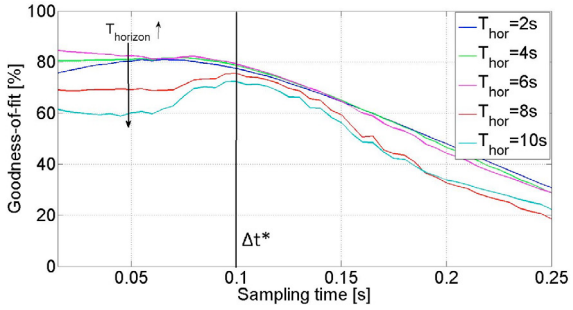

Fig. 8. GoF for different horizon times when γ=250.

period of $T_P = 8$s. Also the required forecast horizon has been set at 10s in Fig. 2. The impulse response caused by a punctual velocity input will produce a force acting on the wet surface of the device: this force will tend to zero with time.

5.1 Order selection for prediction model

The prediction is computed by an autoregressive model, which has a certain order: the higher the order, the more accurate the predictions will be (note that the aliasing problem will appear for higher orders, so a compromise should be reached). In the present work, the degree which provides the best result is n =6, as shown in Fig. 7.

5.2 Optimal selection of sampling time

The sampling time must be defined adequately to avoid aliasing problems (due to too a large sampling time) and excessive computational time (due to too a small sampling time). In Fig. 8, the GoF has been plotted for a determined set of constrained parameters, a certain number of horizon times and a JONSWAP spectrum with peak-shape defined by γ. It can be seen that the goodness-of-fit diminishes when the horizon time increases.

In Fig. 7 the horizon time has been defined, whereas γ gets different values. Increasing γ means reducing the number of frequencies considered, so the GoF of the prediction model increases.

Both parameters, horizon time and peak factor γ, strongly drive the performance of the excitation force prediction model. These factors have been plotted in Fig. 10.

Even if the best GoF is given for an horizon time around 6 s, as seen in Fig. 10. From Fig. 8 and Fig. 9, it can be

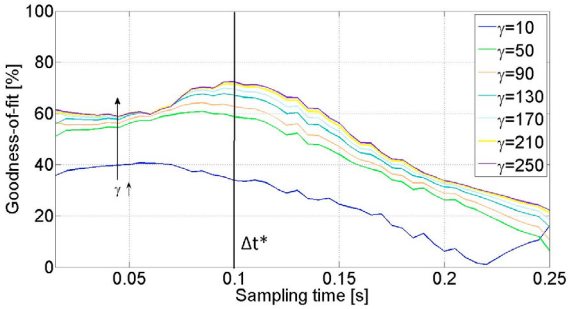

Fig. 9. GoF for different γ when the horizon forecast is 10 s.

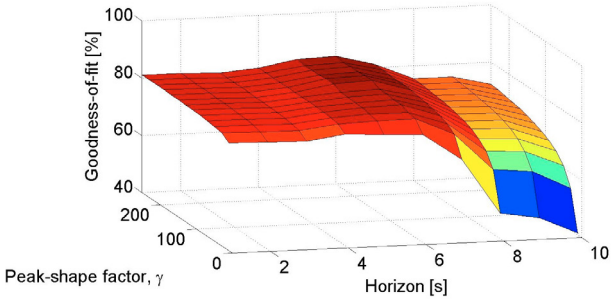

Fig. 10. GoF for variable horizon time and peak-shape factor γ

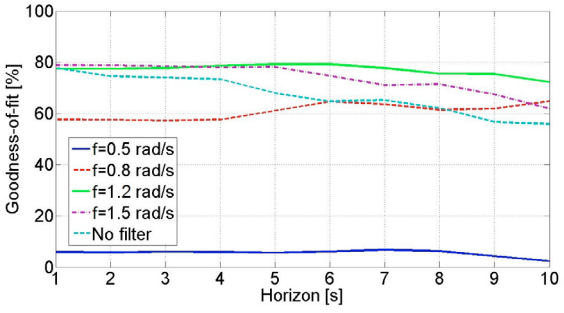

Fig. 11. GoF for different low-pass filters.

derived that the optimal prediction model has a sampling time of 0.1 s, as long as the maximum GoF is around this value for most of the variables.

5.3 Low-pass filtering

Low-pass filtering of the estimated excitation force has been applied (Laurent (2016)). The low-pass filter neglects the high frequencies in the spectrum of the excitation force and, therefore, improves the performance of the prediction model. In Fig. 1 it can be seen that the magnitude of the motion is negligible for frequencies larger than 1.2 rad/s. In Fig. 11 the goodness-of-fit has been shown for different cut-off frequencies of the low-pass filter for a sampling period of 0.1 s and peak shape factor $\gamma = 3.3$. The Chebyshev filter has been applied to filter the excitation force estimate; f represents the filters applied.

A non-casual Chebyshev filter that does not introduce a phase delay has been applied to the estimation of the excitation force in order to eliminate the high frequency components in the signal. A non-casual filter is used

in our paper since the prediction is carried out offline. However, for an online implementation of the prediction of the excitation force, low-pass filtering of the signal will introduce a phase delay which will decrease the accuracy of the prediction.

6. CONCLUSION

This paper attempts to construct the methodology needed to build an excitation force estimator and forecaster. Accurate future excitation force is required in order to implement this knowledge into control strategies, which optimize the energy capture for the WEC.

Along the actual project has been confirmed that several factors could be revised in order to increase the goodness-of-fit between the real and the predicted excitation force: order of the prediction method, sampling time, required forecast horizon and application of a potential low-pass filter.

Note that the methodology shown in the present paper can be applied to new situations, considering extra forces (PTO, moorings systems), different WEC geometries and to an array of WECs.

Further work will focus on the implementation of new optimized parameters: the choices of the number of frequencies, which drives the definition of the wave spectrum and the white noise.

ACKNOWLEDGEMENTS

This paper is based upon works supported by the Science Foundation Ireland under Grant No. 12RC2302 for the Marine and Renewable Energy Ireland (MaREI) centre.

REFERENCES

Abdelkhalik, O., Bacelli, G., Iii, R.D.R., Wilson, D.G., and Coe, R.G. (2016). Estimation of excitation force on wave energy converters using pressure measurements for feedback control. *International Journal of Control*, (October 2016).

Abdelrahman, M., Patton, R., Guo, B., and Lan, J. (2016). Estimation of Wave Excitation Force for Wave Energy Converters. In *15th World Congress of the International Federation of Automatic control*.

Bacelli, G., Balitsky, P., and Ringwood, J.V. (2013). Coordinated Control of Arrays of Wave Energy Devices Benefits Over Independent Control. *IEEE Transactions on Sustainable Energy*, 1–9.

Falcao (2008). Phase control through load control of oscillating-body wave energy converters with hydraulic PTO system. *Ocean Engineering*, 35(3-4), 358–366.

Falnes, J. (2007). A review of wave-energy extraction. *Marine Structures*, 20(4), 185–201.

Fusco, F. and Ringwood, J.V. (2010a). A study on prediction requirements in time-domain control of wave energy converters. *IFAC Proceedings Volumes (IFAC-PapersOnline)*, 372–377.

Fusco, F. and Ringwood, J.V. (2010b). Short-Term Wave Forecasting for time-domain Control of Wave Energy Converters. *IEEE Transactions on Sustainable Energy*, 1(2), 99–106.

Fusco, F. and Ringwood, J.V. (2011). A Model for the Sensitivity of Non-Causal Control of Wave Energy Converters to Wave Excitation Force Prediction Errors. *Proceedings of the 9th European Wave and Tidal Energy Conference*, 1–10.

Fusco, F. and Ringwood, J.V. (2012). A study of the prediction requirements in real-time control of wave energy converters. *IEEE Transactions on Sustainable Energy*, 3(1), 176–184.

Fusco, F. and Ringwood, J.V. (2013). A simple and effective real-time controller for wave energy converters. *IEEE Transactions on Sustainable Energy*, 4(1), 21–30.

Hasselmann, K., Barnett, T.P., Bouws, E., Carlson, H., Cartwright, D.E., Enke, K., Ewing, J.A., Gienapp, H., Hasselmann, D.E., Kruseman, P., Meerburg, A., Muller, P., Olbers, D.J., Richter, K., Sell, W., and Walden, H. (1973). Measurements of Wind-Wave Growth and Swell Decay during the Joint North Sea Wave Project (JONSWAP). *Ergnzungsheft zur Deutschen Hydrographischen Zeitschrift Reihe*, A(8)(8 0), p.95.

Hwang, J.s., Kareem, A., and Kim, W.j. (2009). Estimation of modal loads using structural response. *Journal of Sound and Vibration*, 326(3-5), 522–539.

Kerrigan, E.C. and Ge, M. (2008). Short-term Ocean Wave Forecasting Using an Autoregressive Moving Average Model.

Laurent, Q. (2016). *Estimation and prediction of wave input and system states based on local hydropressure and machinery response measurements*. Ph.D. thesis.

Lewis, F.L., Xie, L., and Popa, D. (2008). *Optimal and Robust Estimation*, volume 1. CRC Press, Boca Raton, 2nd edition.

Ling, B.A. and Batten, B.A. (2015). Real time estimation and prediction of wave excitation force on a heaving body. In *34th International Conference on Ocean, Offshore and Arctic Engineering*, 10.

Monk, K., Conley, D., Lopes, M., and Zou, Q. (2013). Pneumatic Power Regulation by Wave Forecasting and Real-Time Relief Valve Control for an OWC. *10th European Wave and Tidal Energy Conference*, (October 2016).

Nord, T.S., Lourens, E.M., Oiseth, O., and Metrikine, A. (2015). Model-based force and state estimation in experimental ice-induced vibrations by means of Kalman filtering. *Cold Regions Science and Technology*, 111(December 2014), 13–26.

Ochi, M.K. (1998). *Ocean Waves: The Stochastic Approach*. Cambridge University Press, cambridge edition.

Paparella, F., Monk, K., Winands, V., Lopes, M.F.P., Conley, D., and V. Ringwood, J. (2015). Up-wave and autoregressive methods for short-term wave forecasting for an oscillating water column. *IEEE Transactions on Sustainable Energy*, 6(1), 171–178.

Peñalba Retes, M., Giorgi, G., and Ringwood, J.V. (2015). A Review of non-linear approaches for wave energy converter modelling. *11th European Wave and Tidal Energy Conference*, (1), 1–10.

Ringwood, J.V., Bacelli, G., and Fusco, F. (2014). Control, forecasting and optimisation for wave energy conversion. In *IFAC Proceedings Volumes (IFAC-PapersOnline)*, volume 19, 7678–7689. IFAC.

Tobergte, D.R. and Curtis, S. (2013). *WAMIT User Manual*, volume 53.